Voltammetric and Scanning Force Microscopic Investigation of Anthraquinone Films Spontaneously Adsorbed on Ordered Graphite

Truong C. Ta, Vishal Kanda, and Mark T. McDermott*

Department of Chemistry, University of Alberta, Edmonton, AB T6G 2G2, Canada

Received: September 15, 1998; In Final Form: December 7, 1998

Spontaneously adsorbed organic films can drastically influence the electrochemical reactivity of carbon materials. We report here a combined electrochemical and scanning force microscopic (SFM) study of anthraquinone 2,6-disulfonate films adsorbed to ordered graphite electrodes. The cyclic voltammetric signature of adsorbed 2,6-AQDS depends on the bulk solution concentration of the adsorbate. Films formed from lower concentrations (<10 μM) exhibit near ideal voltammetry for a surface-bound redox system while the voltammetry of layers formed from higher concentration solutions (>10 μM) is less ideal and consists of multiple waves. One of these waves is anomalously sharp, characteristic of significant intermolecular interactions within the adsorbate layer. *In situ* SFM images reveal differences in the two-dimensional structure of 2,6-AQDS films on graphite as a function of concentration. High-resolution lateral force images aid in the correlation of the structure of the adsorbate layers with their electrochemical response. We also discuss the inconsistency between the voltammetrically measured surface coverage and that observed in SFM images.

Introduction

Spontaneously adsorbed organic films play a key role in a variety of applications involving the use of carbon materials in electrochemistry. For example, many schemes to modify the surface of solid electrodes chemically have been developed to systematically control the rates and/or selectivity of heterogeneous electron transfer reactions.[1−3] One of the first approaches involved the physical adsorption (physisorption) of electroactive organic molecules to graphite electrodes.[4] The spontaneous adsorption of redox species to graphite electrode surfaces is simpler and more rapid than procedures involving covalent attachment and remains to be widely utilized as a pathway for immobilization and analysis.[5]

The ease by which organic species adsorb to graphite may also limit the use of these materials in electrochemistry. A physisorbed layer of adventitious impurities can govern the reactivity of a carbon electrode, and reports have stressed the importance of an impurity-free carbon surface.[6] For example, adsorbed layers of organic molecules have been shown to influence electron transfer rates at glassy carbon (GC) electrodes.[7] In applications involving biological components, it has been demonstrated that an adsorbed protein film decreases observed currents at GC electrodes.[8] Thus, it is clear that the spontaneous adsorption of thin films can have a significant impact on the design and application of carbon electrodes.

Crucial to interpreting the electrochemical response of a modified carbon surface is a thorough understanding of how the final structure of the interface influences reactivity. Some of the more important parameters that define the interfacial architecture of a physisorbed layer include the coverage, molecular orientation, and two-dimensional arrangement of the immobilized species. Insights into the structure and coverage of electroactive adsorbed layers can be inferred from their voltammetric signature.[4b,9] Vibrational spectroscopic techniques such as infrared[10] and Raman spectroscopy[11] can provide chemical identification as well as orientation information. The details provided by these methodologies, and others, have advanced our understanding of modified electrochemical interfaces but in a somewhat limited sense because they only describe the general population or average behavior of the adsorbed layer. A more complete picture can be obtained by combining macroscopic characterizations with techniques that probe the surfaces on a molecular scale. The family of techniques comprising scanning probe microscopy (SPM) has been widely utilized to examine the nanometer-scale structure of thin organic films on electrode surfaces.[12] We herein describe a combined electrochemical and *in situ* scanning force microscopic (SFM) study of anthraquinone 2,6-disulfonate (2,6-AQDS) films adsorbed to ordered graphite electrodes.

Several recent reports have described the electrochemistry of adsorbed 2,6-AQDS layers.[13−17] Anomalous, yet interesting, voltammetry, consisting of multiple waves and a sharp spike was reported for 2,6-AQDS layers adsorbed to both Hg and pyrolytic graphite (PG) electrodes. Faulkner and co-workers proposed an intermolecular hydrogen-bonded structure as being responsible for the sharp voltammetric feature on Hg.[13] In a combined electrochemical and infrared spectroscopic investigation, Zhang and Anson proposed that 2,6-AQDS initially adsorbs in a flat orientation on PG and reconfigures with increasing time or bulk solution concentration.[15] A more recent report describes the adsorption of 2,6-AQDS to a variety of different carbon electrodes and suggests that surface carbon−oxygen functionality serve as adsorption sites.[18] Due to our interest in the interfacial architecture of modified carbon electrodes, we have extended these previous studies. For 2,6-AQDS spontaneously adsorbed on highly oriented pyrolytic graphite (HOPG) surfaces, we correlate here voltammetric responses with film architectures determined by *in situ* SFM imaging.

Experimental Section

Reagents and Materials. Disodium anthraquinone 2,6-disulfonate (2,6-AQDS) was obtained from Aldrich (Milwaukee,

* Author to whom correspondence should be addressed. Voice: 780-492-3687. Fax: 780-492-8231. E-mail: mark.mcdermott@ualberta.ca.

10.1021/jp983724u CCC: $18.00
Published on Web 02/06/1999

WI) and was twice recrystallized from ethanol. All concentrations of 2,6-AQDS were prepared in 1 M $HClO_4$ (Caledon, Georgetown, Ontario). Water used for rinsing and preparation of all solutions was from a Nanopure (Barnstead, Dubuque, IA) water filtration system. Solutions of pH 4 were prepared by adjusting the pH of a 1 M $NaClO_4$ (Anachemia) solution with drops of 1 M $HClO_4$. Highly oriented pyrolytic graphite (HOPG) was either purchased from Advanced Ceramics Corp. (Lakewood, OH) (ZYB grade) or obtained as a gift from Dr. Arthur Moore at Advanced Ceramics (ungraded).

Electrochemistry. Cyclic voltammetry (CV) experiments were performed using a standard three-electrode cell. A Ag/AgCl (saturated KCl) electrode and a platinum wire were used as the reference and the counter electrode, respectively. HOPG was the working electrode and was cleaved with tape to produce a clean, flat surface before each experiment. The area of the working electrode (0.5 cm^2) was defined by the radius of an inert O-ring. Voltammograms were obtained by sweeping the potential between +0.4 and −0.1 V vs Ag/AgCl at a scan rate of 100 mV/s using a PAR Model 270 potentiostat. Solutions of higher concentration (>100 μM) produce currents arising from both solution and surface-bound species. For these solution concentrations, 2,6-AQDS was allowed to adsorb for ~30 min. The cell was then rinsed with 1 M $HClO_4$, and the experiments were conducted in 1 M $HClO_4$. Similar results were obtained from experiments performed in the microscope's electrochemical fluid cell.

SFM Studies. *In situ* SFM experiments were carried out in the electrochemical fluid cell of a Nanoscope III Multi-Mode system (Digital Instruments, Santa Barbara, CA). Contact mode topographic and lateral force images were collected simultaneously. Typically, the fluid cell was filled with 1 M $HClO_4$ and allowed to equilibrate for at least 30 min. The 2,6-AQDS solutions were then flushed through the fluid cell and allowed to equilibrate with the surface for 30 min. Imaging was performed with minimal load applied to the surface. This was achieved by using a cantilever with a low force constant ($k \approx$ 0.06 N/m, Digital Instruments) and imaging at normal forces <2 nN.

Molecular Modeling. To approximate the molecular dimensions of 2,6-AQDS, we incorporated tabulated van der Waal's radii[19] into commercial modeling software (MacroModel 5.5, MacroModel Development Group, Columbia University).

Results and Discussion

As noted above, several previous reports have described the cyclic voltammetry for 2,6-AQDS adsorbed at various electrode materials.[13−17] Although support for our conclusions here derives mainly from SFM analysis, examples of the voltammetry of 2,6-AQDS adsorbed on cleaved basal plane HOPG from 1 M $HClO_4$ are presented for completeness. In all cases, the voltammetry presented was collected after the adsorbed layer had reached equilibrium with the contacting solution (~30 min). Figure 1A is the current−potential curve collected in a solution of 1.0 μM 2,6-AQDS, a concentration where solution phase species are undetectable by cyclic voltammetry. The voltammetric waves centered at 0.090 V vs Ag/AgCl exhibit a full-width-at-half-maximum (FWHM) of 54 mV and a peak separation (ΔE_p) of 7 mV. The peak current of these waves increases linearly with the voltammetric scan rate. These observations indicate that 2,6-AQDS behaves as a near ideal, quasi-reversible, surface-bound redox species when adsorbed to HOPG from micromolar concentrations.[20] In addition, the position of the waves in Figure 1A is ~0.05 V more positive than the $E_{1/2}$ for diffusing 2,6-AQDS ($E_{1/2}$ = 0.040 V vs Ag/AgCl), implying that the reduced hydroquinone form is more strongly adsorbed. The wave shape and position in Figure 1A are generally observed for 2,6-AQDS adsorbed from solutions of concentrations <10 μM in 1 M $HClO_4$.

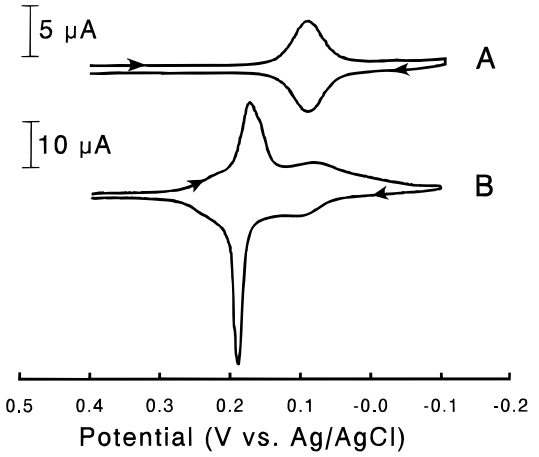

Figure 1. Cyclic voltammetry (CV) of 2,6-AQDS adsorbed on HOPG for 30 min from different solution concentrations: (A) CV in 1 μM 2,6-AQDS (1 M $HClO_4$); (B) CV in 1 M $HClO_4$ after adsorption from 1 mM 2,6-AQDS (1 M $HClO_4$). ν = 100 mV/s for both voltammograms.

Integration of the area under the cathodic wave in Figure 1A yields a charge of 4.5×10^{-6} C/cm^2, which corresponds to an observed surface coverage (Γ_{obs}) of 2.3×10^{-11} mol/cm^2. On the basis of a saturation coverage of 1.32×10^{-10} mol/cm^2, which assumes that the aromatic rings of adsorbed 2,6-AQDS are oriented parallel with the graphite surface (molecular area = 128 Å^2), this coverage reflects ~17% of a fully-packed monolayer.[21] Submonolayer quantities of quinones adsorbed to HOPG have been previously detected by voltammetry. It has been concluded that either 2,6-AQDS adsorbs solely to the area near a defect or adsorbed 2,6-AQDS is electroactive only at defects.[14,16] As described below, our SFM data suggests that the second explanation is more reasonable.

Figure 1B shows the cyclic voltammetry of 2,6-AQDS collected in supporting electrolyte after adsorption to HOPG from a 1.0 mM solution. In addition to the waves at 0.09 V, a second set of peaks develops at 0.19 V vs Ag/AgCl. These spiked-shaped peaks are similar to those observed on Hg[13] and PG[15] electrodes and are not observed for bulk solution concentrations less than 10 μM. We note that in a previous report, Anson et al. observed three waves in the voltammetry of 2,6-AQDS on PG electrodes.[15] We also have observed a third wave in ~30% of our experiments at potentials slightly more negative than the one at 0.09 V. Because of this irreproducibility we do not comment further on this third wave (see note 28).

The presence of multiple waves in Figure 1B argues that 2,6-AQDS adsorbs to HOPG in distinct states. One state, characterized by the well-behaved waves at 0.09 V, appears to be that of a model surface-bound redox species. The FWHM of the spikes in Figure 1B are 37 mV for the cathodic wave and 23 mV for the anodic. These narrow voltammetric waves imply a second adsorbate state exhibiting significant intermolecular interactions.[22] Theoretical treatments by Laviron suggest that the location of the spike as a prewave on the potential axis is also attributable to energy effects arising from the interactions between adsorbed molecules.[23] Integration of the cathodic waves in Figure 1B yields charges of 2.5×10^{-6} μC/cm^2 for the wave at 0.09 V and 1.2×10^{-5} μC/cm^2 for the spike at 0.19 V. The similarity of the charges for the waves at 0.09 V in both

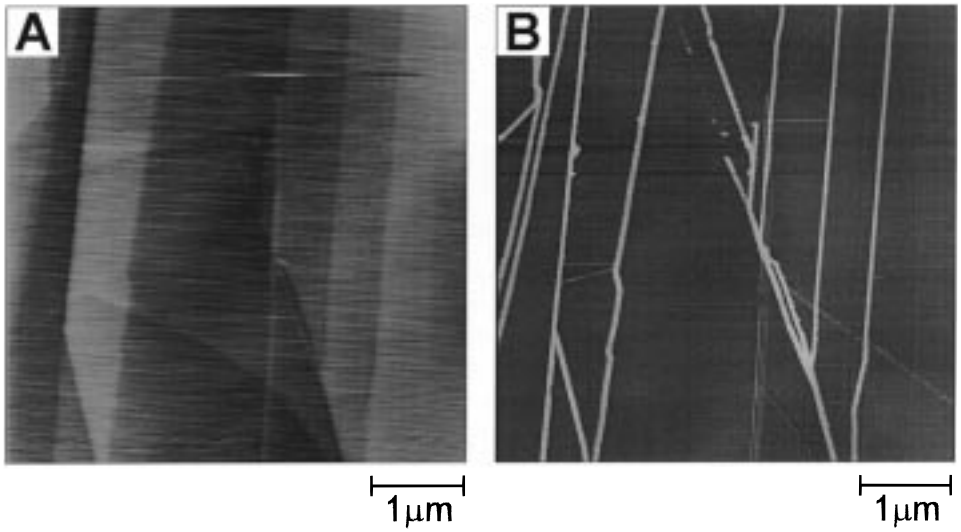

Figure 2. 5 μm × 5 μm SFM images of unmodified HOPG obtained in 1 M $HClO_4$: (A) topography (*Z*-scale = 5 nm); (B) lateral force (*Z*-scale = 0.3 V).

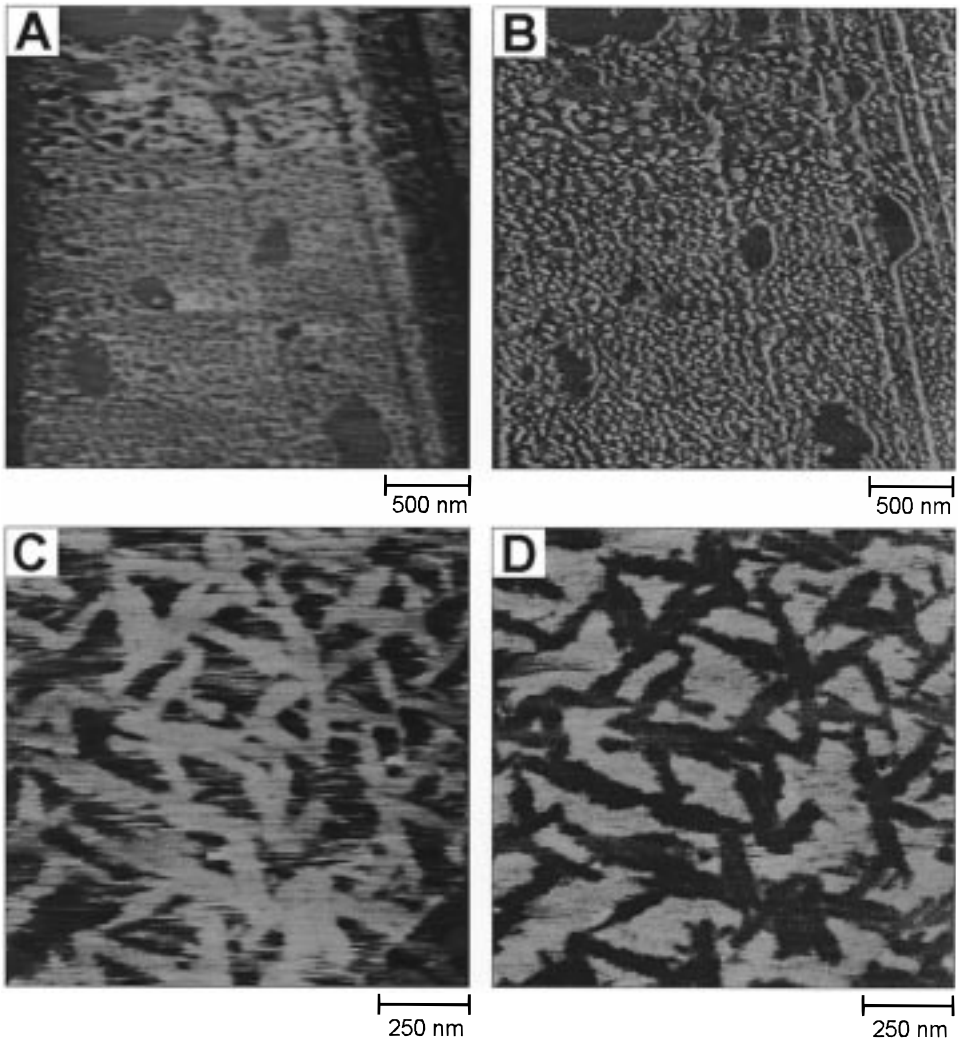

Figure 3. (A) and (B) are respectively 2.7 μm × 2.7 μm topographic (*Z*-scale = 10 nm) and lateral force (*Z*-scale = 0.2 V) SFM images of an equilibrated 2,6-AQDS film on HOPG. Images were collected in 10 μM AQDS (1 M $HClO_4$). (C) and (D) are respectively 1.6 μm × 1.6 μm topographic (*Z*-scale = 2 nm) and lateral force (*Z*-scale = 0.5 V) SFM images collected in 1 mM 2,6-AQDS (1 M $HClO_4$) solution.

voltammograms of Figure 1 suggests that the second adsorbed state does not exist at the expense of the first. Taken together, the voltammetry in Figure 1 illustrates that the structure of spontaneously adsorbed films of 2,6-AQDS on HOPG is governed by the initial bulk concentration. Changes in adsorbed orientation as a function of bulk concentration have been

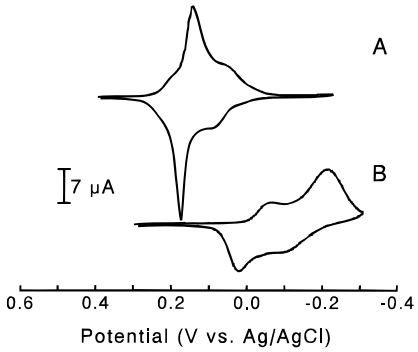

Figure 4. Cyclic voltammetry of 2,6-AQDS films formed from 1 mM AQDS (1 M $HClO_4$) at different pHs: (A) 1 M $HClO_4$, pH $\sim$ 0; (B) 1 M $NaClO_4$ adjusted to pH = 4 with $HClO_4$. ν = 100 mV/s for both voltammograms.

reported for other adsorbate/electrode combinations including 2,6-AQDS on PG[15] and various aromatic molecules on Pt.[24]

The two-dimensional architecture of 2,6-AQDS layers adsorbed to HOPG was investigated with *in situ* contact-mode SFM to better determine the nature of the differences in the cyclic voltammetry observed in Figure 1. The images in Figure 2 are that of unmodified HOPG in 1 M $HClO_4$ and serve to characterize our substrate. The 5.0 $\times$ 5.0 μm topographic (Figure 2A) and lateral (friction) force (Figure 2B) images reveal regions of an atomically flat basal plane separated by step defects created in the cleavage process.[16,25] These steps, which generally exhibit heights corresponding to the interplane distance of graphite (0.33 nm), cause the SFM probe to "trip", resulting in a transient twisting of the cantilever and the observed high lateral force signal at these sites (Figure 2B).[26,27] The images in Figure 2 agree with what we expect on the basis of previous STM[25] and SFM[26] studies of HOPG and provide a signature of the substrate for comparisons with images of 2,6-AQDS layers.

Exposure of a freshly cleaved HOPG surface to solutions of 2,6-AQDS results in the images contained in Figure 3. Parts A and B of Figure 3 are respective 2.7 $\times$ 2.7 μm topographic and lateral force images collected in a 10 μM 2,6-AQDS solution at an imaging force of $\sim$2 nN. Figure 3A reveals topography that is distinct from the unmodified substrate shown in Figure 2A. An apparent overlayer covers approximately 90% of the surface. We note that this type of layer is observed only when imaging under $HClO_4$ solution. Images of HOPG collected in air following exposure to 2,6-AQDS solutions reveal adsorbate only at defect sites. This implies that the interaction of 2,6-AQDS with basal plane graphite is weak relative to the force applied by the scanning probe tip (10$-$50 nN in air). The film topography in Figure 3A appears discontinuous, containing a high density of pinhole defects. In most cases, the diameter of these pinholes is insufficient to allow the SFM tip to probe the HOPG substrate. The tip contacts the edge of the defect, resulting in a high lateral force at these sites due to tripping (Figure 3B). Also apparent are several 100$-$250 nm diameter defects, which display the characteristic low friction (darker contrast) of exposed basal plane in Figure 3B. High-resolution images reveal no observable molecular order in the film structure. Several cleavage steps are present on the right side of Figure 3A,B. We do not observe any differences in film structure near these sites. After examination of a number of such samples, we conclude that the voltammetric wave at 0.09 V in Figure 1A corresponds to the film structure observed in Figure 3A,B.

Consistent with the voltammetry in Figure 1, the structure of 2,6-AQDS films as revealed by SFM varies as a function of bulk concentration. Topographic and lateral force images of basal plane HOPG collected in 1 mM 2,6-AQDS solution are shown in parts C and D of Figure 3, respectively. The topography consists of a pattern of intersecting, elongated domains that are 0.3$-$0.7 nm higher than the surrounding background. These domains range in length from 100 to 700 nm and in width from 35 to 100 nm. Interestingly, in Figure 3D the domains exhibit a significantly lower friction relative to the topographically recessed background. It is not likely, then, that the background consists of basal plane HOPG, which generally displays relatively low friction. The presence of the wave at 0.09 V in Figure 1B suggests that a portion of the overall 2,6-AQDS film structure formed from 1 mM solutions is similar to that in Figure 3A. We thus believe the recessed background in Figure 3C,D consists of this type of structure.

Separate experiments (data not shown) support this supposition and indicate that the domains apparent in parts C and D of Figure 3 are located on top of the initial disordered layer of 2,6-AQDS. A freshly cleaved HOPG surface was exposed to a 1 μM solution in the SFM fluid cell. Images of the resulting layer were very similar to those in Figure 3A,B. A solution of 1 mM 2,6-AQDS was then injected into the cell, resulting in

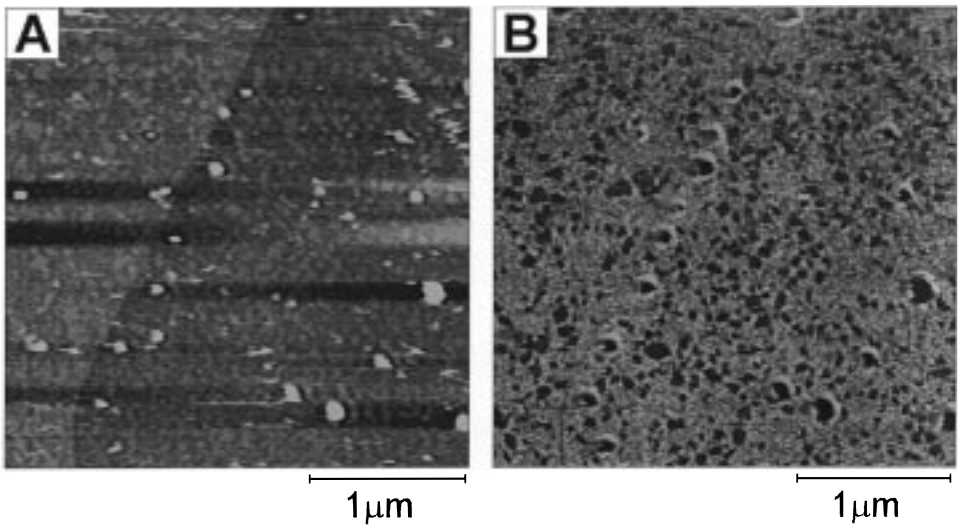

Figure 5. 3 μm $\times$ 3 μm SFM images of 2,6-AQDS film formed from 1 mM 2,6-AQDS (1 M $HClO_4$) collected in 1 M $NaClO_4$ adjusted to pH = 4 with $HClO_4$: (A) topography (Z-scale = 3 nm); (B) friction (Z-scale = 0.1 V).

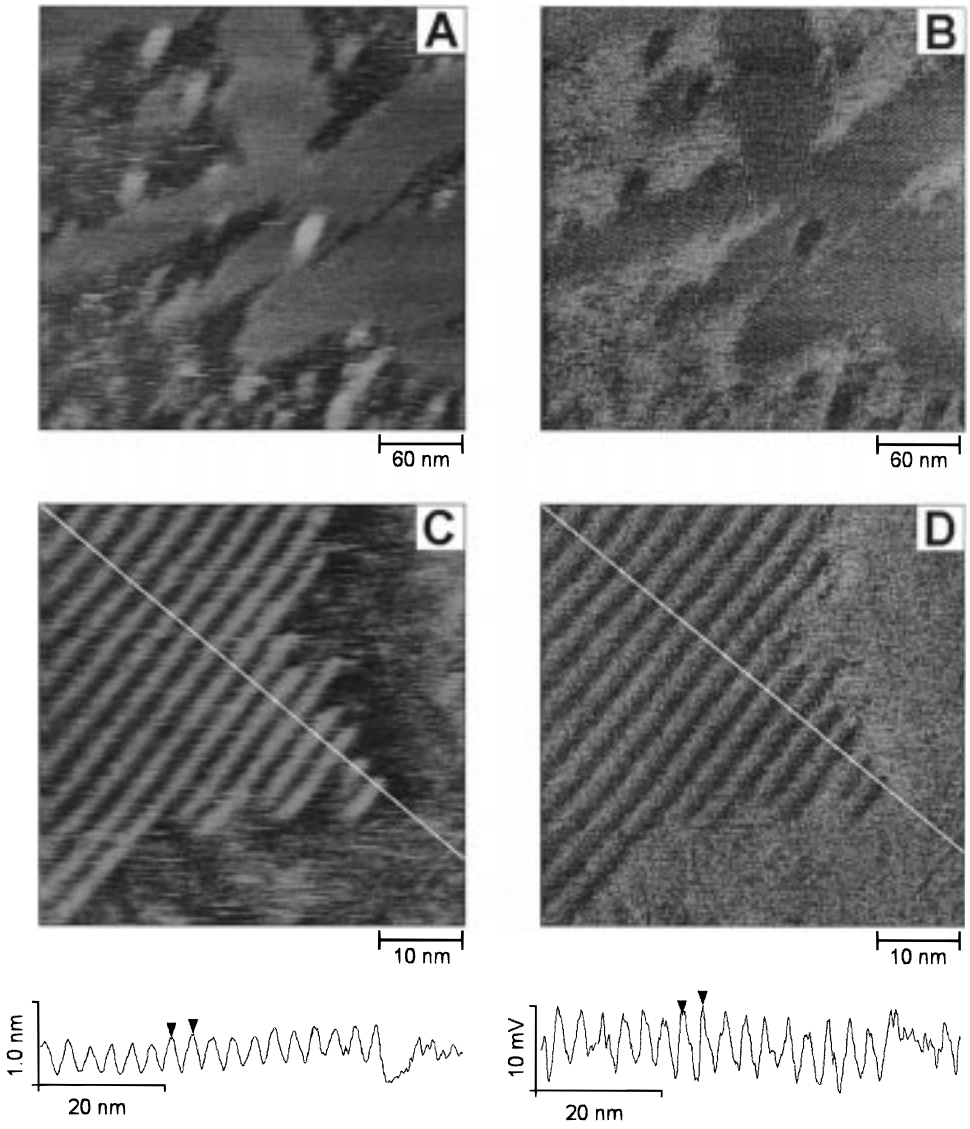

Figure 6. (A) 300 nm × 300 nm topographic (*Z*-scale = 2 nm) and (B) lateral force (*Z*-scale = 0.05 V) SFM images of the domains formed from 1 mM 2,6-AQDS solutions. (C) 50 nm × 50 nm topographic (*Z*-scale = 2 nm) and (D) lateral force (*Z*-scale = 0.05 V) of these domains showing a row-type structure. The cursors in the cross-sectional profiles of (C) and (D) are 3.3 nm apart. All images were collected in 1 mM AQDS (1 M $HClO_4$).

the formation of domains similar to those shown in Figure 3C,D. Furthermore, application of a slightly higher imaging force (~5 nN) causes the domain structures to be swept away, leaving behind the initial disordered layer. These results imply that the observed pattern of domains in Figure 3C is adsorbed on top of the initial, disordered 2,6-AQDS layer observed in Figure 3A,B. Upon initial inspection, the domains in Figure 3C,D appear to intersect at common angles. Angles of 60° or 120° would imply a communication with the underlying graphite lattice. However, analysis of domains in several images does not yield a prevalent angle between domains, which is consistent with a model whereby the domains are separated from the basal plane by another adsorbate layer. Furthermore, on the basis of the combined evidence from the cyclic voltammetry and SFM images, we can assign the spiked voltammetric wave at 0.19 V to the domains that appear only at higher concentrations (>10 μM).

In order to further confirm this assignment, we examined the voltammetry and SFM structure of 2,6-AQDS layers formed from 1 mM solutions as a function of pH. The cyclic voltammogram in Figure 4A was collected under identical conditions and is very similar to that in Figure 1B. Figure 4B is the voltammogram of the same layer after the pH of the electrolyte solution was raised to a value of 4. As expected for an electrochemical reaction involving protons, all waves are shifted to more negative potentials.[20] In addition, the overall charge under the waves in Figure 4B decreases by ~25% relative to that in Figure 4A. This decrease is likely the result of desorption due to the change in pH or rinsing. Importantly, the sharp voltammetric feature observed at lower pH disappeared, consistent with results from a previous report.[15]

A similar experiment was performed in the SFM fluid cell. A cleaved HOPG electrode was exposed to a 1 mM 2,6-AQDS solution, and the resulting film was comparable to that shown in Figure 3C,D. After flushing and filling the cell with pH 4 electrolyte solution, the images in Figure 5 were obtained.[28] As illustrated in the topography (Figure 5A) and particularly in the lateral force image (Figure 5B), the density of the domains appears lower and the structures present are much smaller than those in Figure 3C. The disordered, lower layer appears intact,

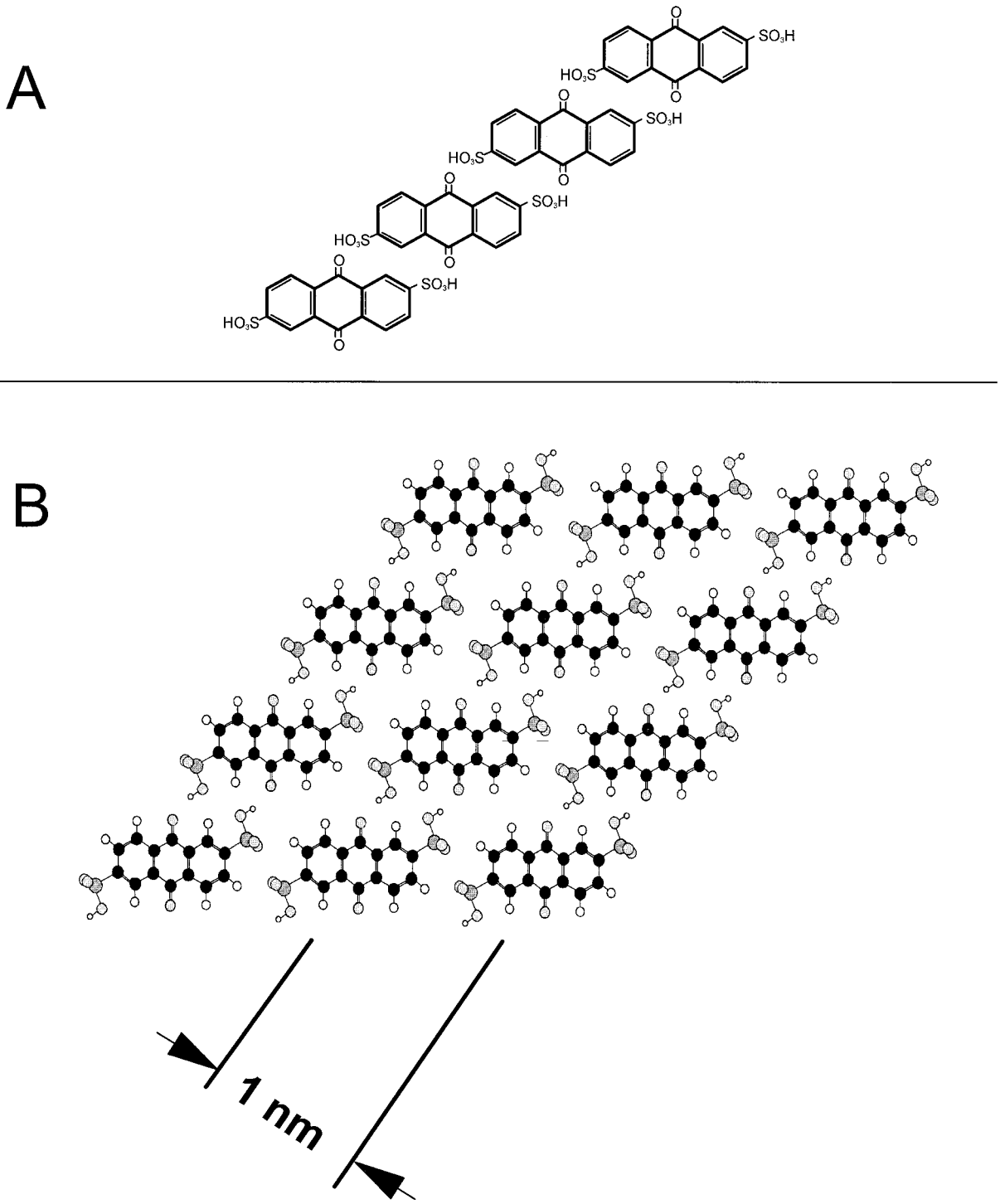

Figure 7. (A) Linear structure originally proposed in ref 13. (B) Predicted row spacing of this structure based on van der Waals radii of 2,6-AQDS.

as evidenced by its relatively high friction in Figure 5B. Considering both the voltammetry in Figure 4B and the images in Figure 5, it is clear that the disappearance of the voltammetric spike correlates with the disassembly of the linear domains. This observation provides strong evidence that the spike is the voltammetric signature of the linear domain structures.

The images in Figure 3, and others that we have obtained during this work, indicate that the vast majority of the cleaved HOPG surface is covered with a layer of 2,6-AQDS when adsorbed from solution concentrations from 1 μM to 1 mM. This observation is inconsistent with the measured voltammetric coverage in Figure 1 (e.g., 17% of a monolayer for Figure 1A) and reported previously.[14,17] In fact, for solution concentrations of 1−10 μM, we have never measured voltammetrically full monolayer coverage of 2,6-AQDS adsorbed to cleaved basal plane HOPG electrodes. It has been demonstrated that the amount of adsorbed 2,6-AQDS on HOPG correlates with the density of edge plane defects.[17] The SFM results presented here suggest that these types of adsorbates may only be *electroactive* at defects, leading to the above-mentioned correlation. Results from a recent study indicate that surface oxygen groups act as sites for the adsorption of 2,6-AQDS on carbon surfaces.[18] It may be that these functionalities are necessary for electron transfer to these adsorbates. In any case, it is clear from the

images in Figure 3 that the amount of 2,6-AQDS actually adsorbed to HOPG electrodes does not agree with the amount determined electrochemically. This discrepancy is currently under investigation.[29]

Insights into the molecular structure of the domains formed from higher concentration solutions of 2,6-AQDS (>10 μM) begin to develop from careful consideration of the lateral force image in Figure 3D. The measured friction in these regions is significantly lower than in the underlying film. Based on recent studies, this observation implies either a variation in chemical composition between the two regions[30] or a difference in molecular packing.[31] As mentioned above, the reduced width of the voltammetric wave corresponding to the domains is indicative of significant intermolecular interactions, which adds weight to the latter of the two scenarios. High-resolution images of the layer depicted in Figure 3A,B reveal no molecular order and are consistent with a greater measured friction and a near ideal voltammetric wave shape. The lower friction and sharp voltammetric signature of the domains argues that significant intermolecular interactions exist and that these regions may be composed of a more ordered array of molecules.

High-resolution SFM images detail further the molecular scale architecture of 2,6-AQDS domains. Parts A and B of Figure 6 are 300 × 300 nm topographic and lateral force images that reveal molecular-scale order in the domains. The domains appear to be composed of parallel, linear rows or stripes. These rows are more apparent in the lateral force image (Figure 6B), likely due to the higher sensitivity of a laser-reflection based SFM to the torsional motion of the cantilever.[32] The stripes are oriented with the long axis of the domains and traverse each domain without interruption. The termination of the stripes occurs either at a free-standing domain edge, at a cleavage defect, or at the boundary between two (or more) domains. The intersection of several domains is illustrated near the center of Figure 6A,B. The boundaries between intersecting domains are well-defined with clean termination of the stripes of one domain into the stripes of another. These boundaries are reminiscent of grain boundaries observed in scanning tunneling microscopy images of liquid crystal monolayers on HOPG.[33] Importantly, the stripe structure observed in Figure 6A,B strongly argues that the domains are ordered on a molecular scale. This conclusion is consistent with the observed low friction and sharp voltammetric wave.

The stripe structure is depicted in greater detail in the 50 × 50 nm images of Figure 6C,D. From the cross-sectional profile in Figure 6C, the periodicity between the stripes measures 3.3 nm with a corrugation amplitude of 0.35 nm. Interestingly, the rows themselves exhibit lower friction than the surrounding layer and it is the combined effect of the group of stripes that produces overall lower friction of the entire domain.[34] Although our SFM images reveal nanometer-scale periodicity, they do not display the resolution necessary to predict the molecular packing scheme responsible for the observed row structure. A hydrogen-bonded structure, originally predicted by Faulker et al.[13] and shown in Figure 7A, would produce rows of interacting molecules. Using van der Waals radii, our modeling efforts yield a sulfonate−sulfonate distance in 2,6-AQDS of 14 Å. On the basis of this distance, the adjacent row spacing for flat-lying molecules would be ~1 nm (Figure 7B), which is much smaller than our measured inter-row distance of 3.3 nm. An edgewise orientation would exhibit an even smaller row−row periodicity. Thus, the large periodicity relative to the dimension of individual 2,6-AQDS molecules suggests that a simple structure involving a string of interacting single molecules is unlikely. In addition, we cannot envision a flat lying structure like that depicted in Figure 7 to exhibit the low friction observed in our experiments. We believe that the low friction of each row reflects a crystalline architecture where the cross-section of each row is composed of a densely packed group of molecules, likely packed via hydrogen bonding. This crystal structure then extends linearly. We are currently exploring the molecular arrangement of the observed row structure with *in situ* scanning tunneling microscopy.

Conclusion

It is clear from our experiments that the two-dimensional structure of 2,6-AQDS films spontaneously adsorbed to HOPG is governed by the solution concentration from which the films are formed. The different film architectures are reflected both in the voltammetric response of the films and in SFM images. When 2,6-AQDS is adsorbed from solutions of 10 μM or less, a near complete, disordered monolayer exhibits near ideal cyclic voltammetry for a surface-bound redox system. This layer apparently adsorbs to the basal plane of the HOPG electrode with no predisposition for binding solely to cleavage defects. An array of molecular domains forms on top of the original disordered layer from solutions of higher concentration (10 μM to 1 mM). The appearance of these domains correlates with the development of a sharp spike in the voltammetry. The width of the spike as well as its location on the potential axis suggests a structure exhibiting significant intermolecular interactions. Two characteristics revealed by SFM imaging confirm this type of structure. First, lateral force images show that the domains exhibit an overall lower friction than the initial disordered film, implying a crystalline architecture. Secondly, high-resolution images reveal that each domain is composed of a series of parallel rows, again pointing to a well-defined, organized structure.

The full coverage of adsorbed 2,6-AQDS observed in SFM image does not correlate with the coverage determined voltammetrically here (~17%) and elsewhere.[14] This suggests that adsorbed 2,6-AQDS is electroactive only at certain sites, likely cleavage defects. The different 2,6-AQDS film architectures reported here can only be observed when imaging under solution. Images collected in ambient air reveal adsorbate only on the cleavage defects. This points to a stronger binding of 2,6-AQDS to edge plane graphite relative to the basal plane and is consistent with preferential electroactivity at these sites. The combination of voltammetric measurements and *in situ* SFM imaging in this work has provided a powerful correlation relating the electrochemical reactivity and two-dimensional structure of spontaneously adsorbed 2,6-AQDS films on graphite.

Acknowledgment. This work was supported by the Natural Sciences and Engineering Research Council of Canada (NSERC) and the Department of Chemistry, University of Alberta. We thank Dr. Arthur Moore for the gift of HOPG and Professor Neil Branda for the use of the computer and software for molecular modeling.

References and Notes

(1) Murray, R. W. In *Electroanalytical Chemistry*; Bard, A. J., Ed.; Marcel Dekker: New York, 1984; Vol. 13, pp 191-368.
(2) Hubbard, A. T. *Chem. Rev.* **1988**, *88*, 633.
(3) Bard, A. J.; et al. *J. Phys. Chem.* **1993**, *97*, 771.
(4) (a) Brown, A. P.; Koval, C.; Anson, F. C. *J. Electroanal. Chem.* **1976**, *72*, 379. (b) Brown, A. P.; Anson, F. C. *Anal. Chem.* **1977**, *49*, 1589. (c) Brown, A. P.; Anson, F. C. *J. Electroanal. Chem.* **1977**, *83*, 203.
(5) See, for example: Shi, M.; Anson, F. C. *Anal. Chem.* **1998**, *70*, 1489.

(6) (a) McCreery, R. L. In *Electroanalytical Chemistry*; Bard, A. J., Ed.; Marcel Dekker: New York, 1991; Vol. 17, pp 221-374. (b) McCreery, R. L.; Kneten, K. R.; McDermott, C. A.; McDermott, M. T. *Coll. Surf. A* **1994**, *93*, 211.

(7) (a) Chen, P.; Fryling, M. A.; McCreery, R. L. *Anal. Chem*. **1995**, *67*, 3115. (b) Chen, P.; McCreery, R. L. *Anal. Chem*. **1996**, *68*, 3958.

(8) (a) Downard, A. J.; Roddick, A. D. *Electroanal.* **1994**, *6*, 409. (b) Downard, A. J.; Roddick, A. D. *Electroanalysis* **1995**, *7*, 376.

(9) Laviron, E. In *Electroanalytical Chemistry*; Bard, A. J., Ed.; Marcel Dekker: New York, 1982; Vol. 12, pp 53-157.

(10) (a) Porter, M. D.; Bright, T. B.; Allara, D. L.; Kuwana, T. *Anal. Chem*. **1986**, *58*, 2461. (b) Porter, M. D. *Anal. Chem*. **1988**, *60*, 1143A.

(11) (a) Zhao, J.; McCreery, R. L. *Langmuir* **1995**, *11*, 4036. (b) Kagan, M. R.; McCreery, R. L *Langmuir* **1995**, *11*, 4041. (c) Liu, Y.-C.; McCreery, R. L. *J. Am. Chem. Soc*. **1995**, *67*, 3115.

(12) Green, J.-B. D.; McDermott, C. A.; McDermott, M. T.; Porter, M. D. In *Frontiers in Electrochemistry: Imaging of Surfaces and Interfaces*; Lipkowski, J., Ross, P. N., Eds. (in press).

(13) He, P.; Crooks, R. M.; Faulkner, L. R. *J. Phys. Chem*. **1990**, *94*, 1135.

(14) McDermott, M. T.; Kneten, K.; McCreery, R. L. *J. Phys. Chem.* **1992**, *96*, 3124.

(15) Zhang, J.; Anson, F. C. *J. Electroanal. Chem.* **1992**, *331*, 945.

(16) Forster, R. J. *Langmuir* **1995**, *11*, 2247.

(17) McDermott. M. T.; McCreery, R. L. *Langmuir* **1994**, *10*, 4307.

(18) Xu, J.; Chen, Q.; Swain, G. M. *Anal. Chem.* **1998**, *70*, 3146.

(19) *CRC Handbook of Chemistry and Physics*; 66th ed.; Weast, R. C., Ed.; CRC Press: Boca Raton, FL, 1985.

(20) Bard, A. J.; Faulkner, L. R. *Electrochemical Methods*; Wiley: New York, 1980.

(21) Soriaga, M. P.; Hubbard, A. T. *J. Am. Chem. Soc*. **1982**, *104*, 3937.

(22) Laviron, E. *J. Electroanal. Chem*. **1974**, *52*, 395.

(23) Laviron, E. *J. Electroanal. Chem*. **1975**, *63*, 245.

(24) (a) Soriaga, M. P.; Wilson, P. H.; Hubbard, A. T.; Benton, C. S. J. *Electroanal. Chem*. **1982**, *142*, 317. (b) Soriaga, Stlckney, J. L.; P. H.; Hubbard, A. T. J. *Electroanal. Chem*. **1983**, *144*, 207.

(25) Chang, H.; Bard, A. J. *Langmuir* **1991**, *7*, 1143.

(26) Baselt, D. R.; Baldeschwieler, J. D. *J. Vac. Sci. Technol. B* **1992**, *10*, 2316.

(27) We note that a high lateral force signal is observed while scanning both up and down a step. This has previously been observed for HOPG and was attributed to the meniscus forces present between the tip and sample when imaging in air.[26] Our images were collected in 1 M $HClO_4$, where meniscus forces are minimized. We attribute the increase in the lateral force signal while scanning down a step observed in Figure 2B to an increase in contact area or an imaging artifact resulting from the transient normal deflection of the cantilever at the step (i.e., error signal).

(28) Also observed in Figure 6A,B are several circular features measuring ~0.9 nm in height that exhibit lower friction than the domains. We observe these structures in ~30% of the images collected in this work and believe that they are three-dimensional aggregates of 2,6-AQDS. We also believe that these structures are responsible for a third voltammetric wave that we observe occasionally.

(29) We have imaged adsorbate-covered step defects under potential control. While scanning the potential of the HOPG through the voltammetric wave at 0.09 V vs Ag/AgCl, we observe no discernable variation in the topography or friction of the 2,6-AQDS layer at the defect (Ta, T.; McDermott, M. T. Unpublished results).

(30) (a) Overney, R. M.; Meyer, E.; Frommer J.; Brodbeck, D.; Lüthi, R.; Howald. L.; Güntherodt, H.-J.; Fujihira M.; Takano, H.; Gotoh, Y. *Nature* **1992**, *359*, 133. (b) Frisbie, C. D.; Rozsnyai, L. F.; Noy, A.; Wrighton, M. S. Lieber, C. M. *Science* **1994**, *265*, 2071. (c) Wilbur, J. L.; Biebuyck, H. A.; MacDonald, J. C.; Whitesides, G. M. *Langmuir* **1995**, *11*, 825. (d) Green, J.-B.; McDermott, M. T.; Porter, M. D.; Siperko, L. M. *J. Phys. Chem.* **1995**, *99*, 10960.

(31) McDermott, M. T.; Green, J.-B., D.; Porter, M. D. *Langmuir* **1997**, *13*, 2504-2510.

(32) Meyer, G.; Amer, N. M. *Appl. Phys. Lett*. **1990**, *57*, 2089.

(33) (a) Frommer, J. *Angew. Chem. Int. Ed. Engl*. **1992**, *31*, 1298. (b) Patrick, D. L.; Cee, V. J.; Prurcell, T. J.; Beebe, T. B., Jr. *Langmuir* **1996**, *12*, 1830.

(34) We do not observe any significant variations in the friction of the domains as a function of domain orientation relative to the scan direction.